J. Phys. C: Solid State Phys., Vol. 6, 1973. Printed in Great Britain. © 1973

Cubic–tetragonal–orthorhombic–rhombohedral ferroelectric transitions in perovskite potassium niobate: neutron powder profile refinement of the structures

A W Hewat

Materials Physics Division, AERE, Harwell, Berkshire, UK

Received 19 March 1973

Abstract. The orthorhombic and rhombohedral structures of ferroelectric potassium niobate have been determined by neutron diffraction measurements on powdered crystals, using the profile refinement technique to analyse the data. In the orthorhombic phase at 22 °C the atomic displacements along [011] from the cubic perovskite positions are $\delta(K) = -0{\cdot}006 \pm 9$ Å, $\delta(Nb) = 0{\cdot}070$ Å, $\delta(O_I) = -0{\cdot}138 \pm 6$ Å and $\delta(O_{II}) \equiv \delta(O_{III}) = -0{\cdot}125 \pm 4$ Å. In the rhombohedral phase at 230 K, the displacements are along [111]; $\delta(K) = -0{\cdot}013 \pm 32$ Å, $\delta(Nb) = 0{\cdot}078$ Å and $\delta(O_I) \equiv \delta(O_{II}) \equiv \delta(O_{III}) = -0{\cdot}140 \pm 4$ Å. As a check on the profile technique, the tetragonal structure was redetermined, and good agreement obtained with the previous single-crystal work, with displacements along [001] of $\delta(K) = -0{\cdot}014 \pm 26$ Å, $\delta(Nb) = 0{\cdot}063$ Å, $\delta(O_I) = -0{\cdot}117 \pm 4$ Å and $\delta(O_{II}) \equiv \delta(O_{III}) = 0{\cdot}099 \pm 3$ Å. All of these transitions result from the condensation at $\boldsymbol{q} = 0$ of soft modes in which almost rigid oxygen octahedra vibrate against the potassium and niobium atoms. Our results account for the observed changes in the spontaneous polarization of potassium niobate, and demonstrate the power of the profile refinement technique for the investigation of structural phase transitions.

1. Introduction

In an earlier paper (Hewat 1973a) the cubic–tetragonal ferroelectric structural transition of $KNbO_3$ was attributed to the condensation of a soft lattice vibrational mode in which rigid oxygen octahedra vibrate against the potassium and niobium atoms. The rigidity of these octahedra was ascribed to the strength of the oxygen–oxygen bonds compared with those between potassium–oxygen and niobium–oxygen. In this second paper we show that in the lower-temperature tetragonal–orthorhombic and orthorhombic–rhombohedral transitions the oxygen octahedra remain rigid; the directions of their displacement are along [001], [011] and [111] in the tetragonal, orthorhombic and rhombohedral phases respectively. These lower-temperature structural transitions can also be attributed to the condensation of soft lattice vibrational modes.

The magnitudes and directions of these atomic displacements account for the observed changes in the spontaneous polarization of $KNbO_3$ when the effective atomic charges are estimated from infrared and dielectric data. With these displacements, Cochran's (1960) soft-mode theory of ferroelectricity yields good values for the Curie constants describing the temperature dependence of the dielectric constants.

The second object of this paper is to demonstrate the power of the profile refinement method for the analysis of neutron powder diffraction data for materials undergoing structural transitions. The small atomic displacements which occur ($\sim 0{\cdot}1$ Å) can be measured to $\pm 0{\cdot}005$ Å, the changes in the cell dimensions to $\pm 0{\cdot}0005$ Å, and the changes in the cell angles to $\pm 0{\cdot}01°$. This matches the precision obtainable with conventional single-crystal measurements, but the experiment is much easier, less time-consuming, and allows for greater freedom for changes of external conditions such as temperature and pressure. Since a complete set of data can often be collected in one day, compared with the several weeks usually required for single-crystal neutron work, the possibility of studying a whole series of materials under a variety of conditions is created. In a forthcoming paper we will show how this method can be extended to structural transitions in more complex hydrogen-bonded materials ($NH_4H_2PO_4$ and $NH_4H_2AsO_4$).

2. The profile refinement technique for neutron powder diffraction patterns

Single-crystal neutron diffraction experiments are particularly difficult for $KNbO_3$ and other ferroelectric materials. Unless a large single-domain crystal (5–50 mg) can be grown, it is usually necessary to maintain an electric field of about 10000 V cm^{-1} along the ferroelectric axis in order to align all of the domains (eg Hewat 1973a).

On the other hand, it is a simple matter to obtain a diffraction pattern from a powdered crystal: nothing can be done to align the crystallites in a powder, and the diffraction pattern is merely a function of the scattering angle, all of the reflexions for a given scattering angle being superimposed. The difficulty is in the analysis of these complicated patterns. For a low-symmetry structure differing only slightly from a higher-symmetry 'aristotype'† there may be no well-resolved single peaks at all, since each of the reflexions for the aristotype is split when the symmetry is lowered, the splitting often being below. the resolution limits of the diffractometer. These split peaks contain, though, most of the information about the atomic displacements from the aristotype structure.

Rietveld (1969) has shown that the maximum amount of information can be extracted from these overlapping reflexions by departing from the conventional methods of crystal structure refinement. Instead of attempting to measure the structure factor or intensity for each reflexion, an attempt is made to fit the detailed shape, or profile, of the whole pattern using a structural model for which the atomic positions can be varied according to a least-squares procedure.

The quantity to be minimized is the familiar χ^2 sum:

$$\chi^2 = \sum_i \frac{[y_i(\text{obs}) - y_i(\text{calc})]^2}{y_i(\text{calc})}.$$

This sum is over the squares of the differences between the calculated y_i(calc) and observed y_i(obs) counts at each 2θ point i in the pattern, with an effective weighting factor of σ_i^{-2} where $\sigma_i = \sqrt{\{y_i(\text{calc})\}}$ is the standard deviation expected for the count y_i(obs). The parameters to be refined fall into two groups: those describing the characteristics of the diffractometer and those describing the crystal structure.

The first group consists of the counter zero-point Z, the neutron wavelength λ, and the three parameters U, V, W describing the variation with scattering angle 2θ of the

† 'aristotype' refers here to the ideal cubic perovskite structure.

halfwidth H of the gaussian curve which is used to describe each reflexion,

$$H^2 = U \tan^2\theta + V \tan\theta + W.$$

The calculated profile is just the sum of all these gaussian curves whose positions and heights are calculated from the structural model parameters. At scattering angles greater than $2\theta \sim 30°$, a single reflexion is described quite precisely by such a gaussian curve (Rietveld 1969), but at low angles a slight asymmetry is introduced because of the non-zero height of the powder specimen. Rietveld introduces another parameter P to describe this asymmetry. These instrument-dependent parameters can be determined for a given diffractometer geometry using a standard specimen, but in practice they are usually refined along with the structural parameters.

These structural parameters are the scale factor, the lattice dimensions and angles $(a, b, c, \alpha, \beta, \gamma)$, the fractional coordinates $x(\kappa), y(\kappa), z(\kappa)$ for each atom κ, and isotropic thermal vibrational parameters $B(\kappa)$. Recent modifications to the program (Hewat 1973b) allow the refinement of anisotropic temperature factors $B_{ij}(\kappa)$ as well. All these parameters can be refined within the constraints imposed by the symmetry of the atom positions. In fact any number of linear or quadratic relations between the parameters can be used as constraint functions. Finally, a parameter G can be refined to take account of any preferred orientation of the powder grains; this is a much smaller problem for neutrons than for x-rays, and can safely be neglected in the present work.

3. The cubic–tetragonal transition in $KNbO_3$

As a test of the profile refinement technique for this type of problem, we first applied it to the cubic–tetragonal transition in $KNbO_3$, which has recently been studied by the conventional single-crystal neutron diffraction method (Hewat 1973a). Above the transition temperature of 435 °C, $KNbO_3$ has the aristotype cubic perovskite structure, with K at (000), Nb at $(\frac{1}{2}\frac{1}{2}\frac{1}{2})$ and O at $(\frac{1}{2}\frac{1}{2}0)$, $(\frac{1}{2}0\frac{1}{2})$ and $(0\frac{1}{2}\frac{1}{2})$ on a unit cell of ~ 4 Å. At the transition, the space group changes from $Pm3m$ (No 221) to $P4mm$ (No 99), and the atoms are displaced by $\sim 0{\cdot}1$ Å, producing on each of the unit cells an electrical dipole along one of the cube axes [001]. The new atom coordinates are

$$\text{K at } 0, 0, \Delta(\text{K})$$

$$\text{Nb at } \tfrac{1}{2}, \tfrac{1}{2}, \tfrac{1}{2} + \Delta(\text{Nb})$$

$$\text{O}_\text{I} \text{ at } \tfrac{1}{2}, \tfrac{1}{2}, \Delta(\text{O}_\text{I})$$

$$\text{O}_\text{II} \text{ at } \tfrac{1}{2}, 0, \tfrac{1}{2} + \Delta(\text{O}_\text{II})$$

$$\text{O}_\text{III} \text{ at } 0, \tfrac{1}{2}, \tfrac{1}{2} + \Delta(\text{O}_\text{II}).$$

The origin is determined by the requirement that the centre of mass cannot move in the transition, ie

$$m_\text{K}\Delta(\text{K}) + m_\text{Nb}\Delta(\text{Nb}) + m_\text{O}(\Delta(\text{O}_\text{I}) + 2\Delta(\text{O}_\text{II})) = 0.$$

This equation fixes one of the displacements (we chose $\Delta(\text{Nb})$) in terms of the others. It is the object of the experiment to measure these displacements and to relate them to the condensation of a soft lattice vibrational mode as required by Cochran's (1960) theory of ferroelectricity.

About 20 g of Puratronic grade 1 $KNbO_3$ powder was obtained from Johnson

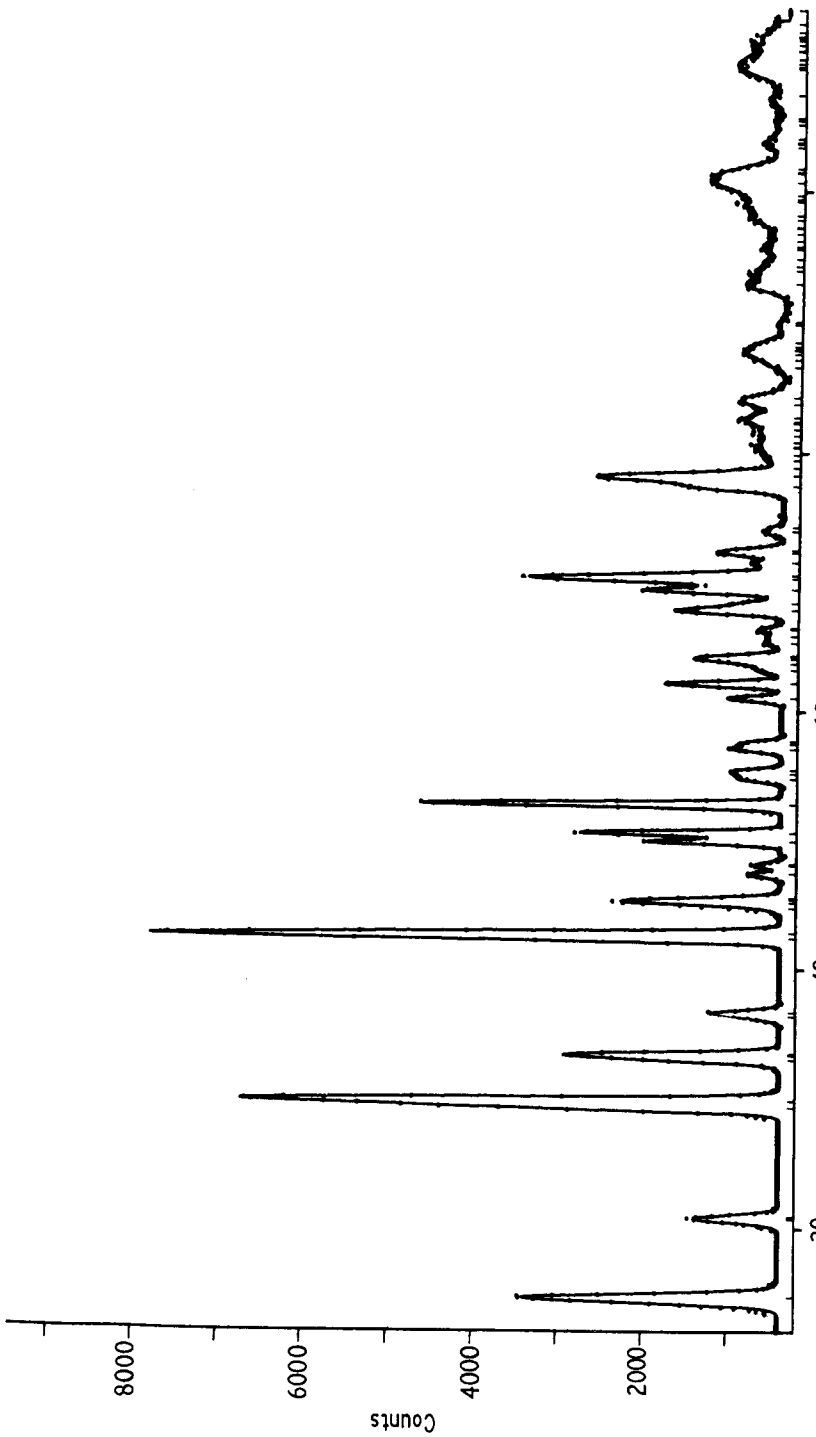

Figure 1. Observed (points) and calculated powder profiles (lines) for tetragonal potassium niobate at 270°C for neutrons of wavelength $\lambda = 1{\cdot}0332$ Å. The positions of the separate reflexions are marked along the 2θ (scattering angle) axis. At high angles these reflexions overlap to such an extent that the profile becomes continuous and complex instead of a series of easily identifiable peaks. At low angles, some of the peaks are broadened by overlap, and on examination of larger-scale drawings, other effects of overlap on the peak shape, such as increased asymmetry, become apparent (eg the third peak in this profile). Those regions of the scan to which no reflexions contribute, drawn as heavy base lines, have been used to measure the background level.

Matthey Chemicals Limited (batch No S 50036: analysis yielded Na = 2, Ca = 1, Mg < 1 parts per million, and no detectable anion impurities). This powder, in a silica-glass tube of diameter 1·5 cm and length 4 cm, was held at 270 °C in the PANDA vacuum furnace during the data collection. The 4 cm diameter tungsten heating element of this furnace produces a single strong peak in the powder pattern at $2\theta = 25°$. This furnace peak has been subtracted from the profile (figure 1) obtained in 22 hours on the PANDA diffractometer at Harwell, using a take-off angle of ~50° to give a wavelength of 1·0332 Å from the (331) plane of the germanium monochromator. The background level was measured in the region of the heavy horizontal lines on this plot, and linearly interpolated and extrapolated for the other regions of the pattern. It is important to be able to measure the scattering angle for each point to at least ±0·1°, since the refinement procedure is extremely sensitive to errors in the peak positions. This precision is possible because of the Moiré fringe method used for positioning the counter on the PANDA diffractometer, which was programmed to make steps of 0·02° and to print out the count at intervals of 0·10° 2θ.

The refinement was started from several different models involving various combinations of signs for the displacements $\Delta(\kappa)$. In this way the final solution was shown to be independent of the starting model. The lattice parameters, counter zero-point, half-width parameters and asymmetry parameter were refined from the start, together with the structural parameters and isotropic temperature factors, without introducing any additional parameter correlation problems. Slightly more precise values for the parameters were actually obtained when the region $2\theta < 59°$ was excluded from the refinement, presumably because small errors remained in the subtraction of the furnace background. The minimum R-factor of 4·33 quoted in table 1 corresponds to the R-factor for integrated intensities

$$R_I = 100 \sum |I(\text{obs}) - I(\text{calc})| / \sum I(\text{obs}).$$

This is approximately twice the R factor for structure factors, R_F, usually quoted for single crystal work. Even with isotropic temperature factors then, we can approach the fit obtained for the single-crystal experiment ($R = 3·8$); moreover the structure parameters obtained for the two experiments agree within the estimated standard deviations σ_p. For the powder work

$$\sigma_p = \left\{ \frac{M_{pp}^{-1}}{N - P + C} \sum \left(\frac{[y(\text{obs}) - y(\text{calc})]^2}{y(\text{calc})} \right) \right\}^{1/2}$$

where M_{pp}^{-1} is the diagonal element of the inverted normal matrix corresponding to the pth parameter, N the number of statistically independent observations, P the number of least-squares parameters, and C the number of constraint functions. Finally, when the temperature factors were permitted to become anisotropic, the fit was improved to $R = 3·7$, matching the single-crystal fit.

It might appear surprising that the precision with which the c/a ratio is determined by the neutron powder data approaches that which is possible with x-ray methods. It is usually thought that the relatively poor resolution of neutron diffractometers should make them very uncompetitive for such measurements. We have already pointed out though, that the profile refinement technique is very sensitive to the positions of the peaks in the powder pattern, and therefore it must also be sensitive to changes in the lattice dimensions. Neutron power diffractometers have an advantage over x-ray instruments in that because of the relatively uncomplicated scattering geometry and radiation spectrum, the line profile is a simple gaussian whose halfwidth can be described over a large range of scattering angles by an equally simple function of θ. This contrasts with

Table 1. Powder results for the tetragonal *P4mm* phase at 270 °C compared with those for the single crystal experiment. $R_I = 100\Sigma_h|I_h(\text{obs}) - I_h(\text{calc})|/\Sigma_h I_h(\text{obs})$ is the *R*-factor for the integrated reflexion intensities, $\Delta_z(\kappa)$ the atomic displacements from the aristotype positions in fractions of the cell edge $c = 4{\cdot}063$ Å, $B_{jj}(\kappa) = 8\pi^2\langle U_{jj}(\kappa)^2\rangle$ the Debye–Waller temperature factors, b_κ the atomic scattering lengths, N_{param} the number of parameters including *U*, *V*, *W*, *Z*, λ and *S*, and Correl—the largest correlation coefficient (maximum 1·0). The powder profile refinement gives more precise results, and the powder data can be collected in one day compared with six weeks for the single-crystal work.

	Single-crystal, neutron $\lambda = 1{\cdot}143$ Å			Powder, neutron $\lambda = 1{\cdot}0332$ Å					
				Isotropic $B(\kappa)$	Anisotropic $B_{jj}(\kappa)$				
$R_I \simeq 2R_F$	3·8			4·3	3·7				
Δ_z(K)	0·023 ± 10			0·018 ± 3	0·018 ± 6				*c*Å
Δ_z(Nb)	0			0	0				*c*Å
$\Delta_z(O_I)$	0·040 ± 3			0·040 ± 1	0·044 ± 1				*c*Å
$\Delta_z(O_{II})$ $\equiv \Delta_z(O_{III})$	0·042 ± 3			0·041 ± 1	0·040 ± 1				*c*Å
	B_{11}	B_{22}	B_{33}	$B(\kappa)$	B_{11}	B_{22}	B_{33}	$\bar{B}_{jj}(\kappa)$	
B_{jj}(K)	1·66 ± 39	1·66	1·18 ± 47	1·16 ± 5	1·04 ± 16	1·04	1·26 + 26	1·11	Å²
B_{jj}(Nb)	0·79 ± 16	0·79	0·24 ± 16	0·55 ± 3	0·67 ± 6	0·67	0·31 ± 16	0·55	Å²
$B_{jj}(O_I)$	0·95 ± 24	0·95	1·26 ± 47	1·06 ± 7	1·18 ± 10	1·18	0·58 ± 21	0·98	Å²
$B_{jj}(O_{II})$	0·87 ± 24	0·79 ± 8	1·26 ± 45	0·73 ± 4	0·99 ± 10	0·45 ± 6	1·00 ± 10	0·81	Å²
$B_{jj}(O_{III})$	0·79	0·87	1·26	0·73	0·45	0·99	1·00	0·81	Å²
c/*a*	1·0165			1·01685 ± 35	1·01687 ± 35				
b_K	0·37			0·37	0·36 ± 2				
b_{Nb}	0·69			0·69	0·69 ± 2				
b_O	0·577			0·577	0·58				
N_{param}	14			14	20				
Correl	0·89 (between Δ(K) and B_{33}(Nb))				0·84 (between Δ(K) and B_{33}(Nb))				
Time	6 weeks			1 day	1 day				

the complex expressions needed to describe x-ray line profiles (Wilson 1963). The profile refinement technique makes it possible, then, for neutron diffractometers to rival x-ray diffractometers for the measurement of changes in the lattice dimensions and angles produced by thermal expansion or structural transition. Further improvements can be expected if future neutron powder instruments are specially designed to take full advantage of the profile refinement technique.

For both the single crystal and powder refinements the displacement Δ(K) of the potassium atom is least well determined because of the relatively high correlation between Δ(K) and B_{33}(Nb) (0·89 for the single crystal refinement and 0·84 for the powder work). This correlation is apparently characteristic of all neutron investigations of the structure, whether they be single-crystal or powder work. Fortunately it is not so important to know Δ(K) precisely, since in the equations for the spontaneous polarization and Curie constant Δ(K) is multiplied by the apparent atomic charge or the square of the atomic mass, both of which are relatively small for potassium (Hewat 1973a).

The estimated errors in the parameters are actually smaller for the powder work. This might be attributed to the absence of systematic errors in the powder pattern, such as those introduced by extinction effects in single-crystal measurements. These systematic errors make it especially difficult to determine precise values for the temperature parameters from single-crystal data. Since these *B*-factors appear to be more precisely determined by the powder data, it is interesting to speculate about the physical reason for the large anisotropy obtained for the vibrational amplitudes of the oxygen atoms.

These atoms appear to have almost twice the mean-square displacement in the plane of the aristotype cube face as they have perpendicular to this plane (eg $B_{11}(O_I) \equiv B_{22}(O_I) \simeq 2B_{33}(O_I)$). Comparison of selected single crystal reflexions for the cubic phase of K(Ta, Nb)O_3 also indicates this kind of anistropy (Hewat 1972); it was attributed then to low-frequency rotations of the rigid oxygen octahedra. Such rotations correspond to zone-boundary optic modes, which are known to be unstable for this structure from lattice-dynamical calculations (Cowley 1964). Indeed in $NaNbO_3$ these modes condense to produce complex superlattice structures (eg Glazer and Megaw 1972). We are unable to find the corresponding superlattice reflexions in the powder patterns for $KNbO_3$, but these zone-boundary modes would produce the observed anisotropy in the mean-square displacements of the oxygen atoms.

4. The tetragonal–orthorhombic transition

The two soft modes degenetate with the mode responsible for the cubic–tetragonal transition are stabilized by this transition, until at 225 °C one of them condenses to give a net polarization along [011] in the orthorhombic phase, when the space group changes to *Amm*2 (No 38). Katz and Megaw (1967) have refined the atomic displacements for this phase from single-crystal x-ray data. The purpose of the present experiment is to measure

Table 2. Powder results for the orthorhombic *Amm*2 phase at 22 °C, compared with those for the single-crystal x-ray experiment (Katz and Megaw 1967). Symbols are as defined in table 1, except that now $\Delta_z(\kappa)$ is along the [011] direction of the aristotype, $\Delta_y(\kappa)$ along [01$\bar{1}$], and $b \simeq c \simeq a\sqrt{2}$ Å, where $a = 3{\cdot}971$ Å. The agreement is satisfactory considering the difficulties of the single-crystal method, where the standard errors have perhaps been underestimated: some parameters are not available (NA) for this x-ray work. The oxygen octahedron is effectively undistorted, since $\Delta_z(O_{II}) \simeq \Delta_z(O_I)$.

	Single crystal, x-ray $\lambda = 0{\cdot}712$ Å			Powder, neutron $\lambda = 1{\cdot}0375$ Å					
				Isotropic $B(\kappa)$	Anisotropic $B_{jj}(\kappa)$				
$R_I \simeq 2R_F$	19·4			2·35	2·11				
Δ_z(K)	0·017 ± 1			0·0132 ± 16	0·0138 ± 71				cÅ
Δ_z(Nb)	0			0	0				cÅ
$\Delta_z(O_I)$	0·021 ± 2			0·0375 ± 8	0·0364 ± 10				cÅ
$\Delta_z(O_{II})$	0·035 ± 2			0·0336 ± 5	0·0342 ± 9				cÅ
$\Delta_y(O_{II})$	0·004 ± 2			−0·0011 ± 5	−0·0024 ± 9				bÅ
	B_{11}	B_{22}	B_{33}	$B(\kappa)$	B_{11}	B_{22}	B_{33}	$\bar{B}_{jj}(\kappa)$	
B_{jj}(K)	NA	0·76 ± 2	0·70 ± 2	0·61 ± 5	0·52 ± 11	0·63 ± 24	0·71 ± 36	0·62	Å^2
B_{jj}(Nb)	NA	0·49 ± 2	0·55 ± 2	0·30 ± 3	0·38 ± 5	0·33 ± 11	0·15 ± 28	0·29	Å^2
$B_{jj}(O_I)$	NA	0·68 ± 6	1·36 ± 25	0·33 ± 6	0·12 ± 7	0·63 ± 20	0·80 ± 35	0·52	Å^2
$B_{jj}(O_{II})$	NA	0·83 ± 6	0·95 ± 14	0·56 ± 4	0·69 ± 5	0·47 ± 12	0·30 ± 21	0·49	Å^2
$B_{jj}(O_{II})$	NA	0·83	0·95	0·56	0·69	0·47	0·30	0·49	Å^2
$B_{23}(O_{II}) = -B_{23}(O_{III})$			−0·17 ± 5				0·14 ± 12		Å^2
b/a	1·4347			1·4336 ± 3	1·4335 ± 3				
c/a	1·4407			1·4402 ± 3	1·4402 ± 3				
b_K	—			0·367 ± 3	0·367 ± 3				
b_{Nb}	—			0·703 ± 4	0·703 ± 4				
b_O	—			0·58	0·58				
N_{param}	NA			19	28				
Time	NA			1 day	1 day				

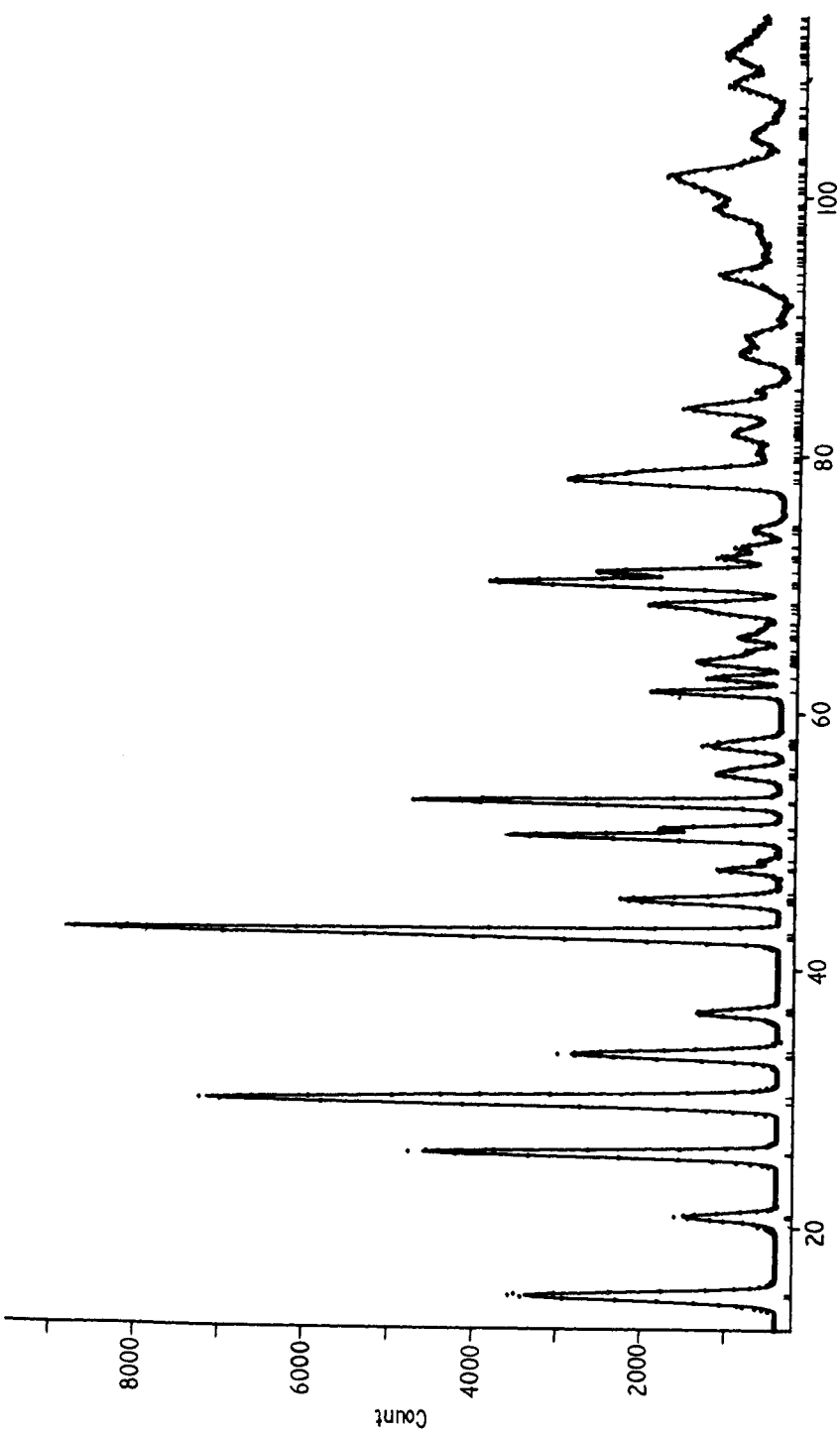

Figure 2. Observed and calculated profiles for orthorhombic potassium niobate at 22°C for a neutron wavelength of 1·0375 Å. The count scale is not precisely the same as for the tetragonal phase, since the data were collected at a different time and under slightly different circumstances (see text). The differences between the profiles for the two phases become quite apparent above $2\theta \sim 47°$. There are now more than 200 separate reflexions marked on the 2θ axis.

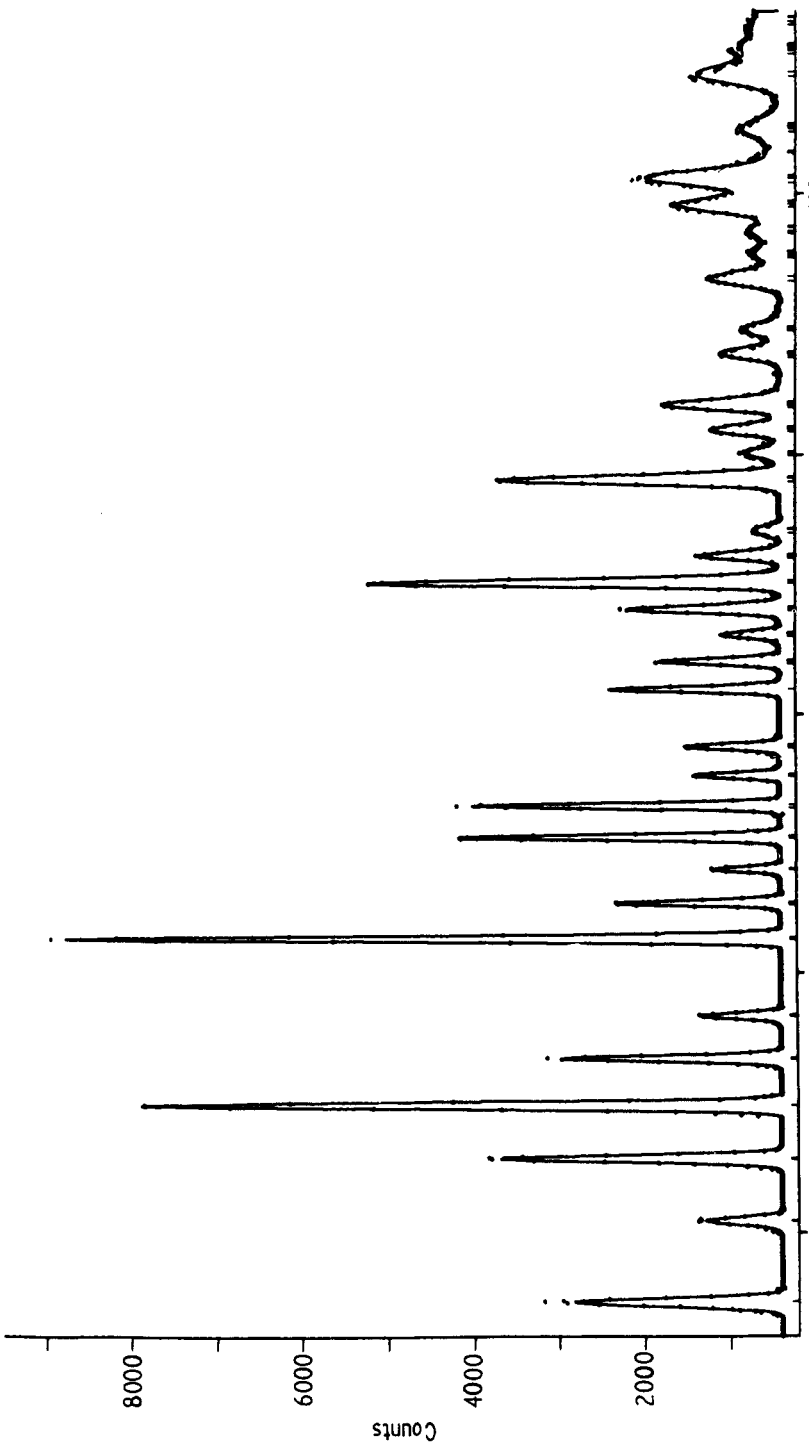

Figure 3. Observed and calculated profiles for rhombohedral potassium niobate at 230 K under the same conditions as for the orthorhombic phase. This profile is simpler than those for the other phases since most of the obvious splitting of the peaks has disappeared. In fact this profile begins to resemble that for the cubic phase, except for systematic changes in the positions and heights of the peaks. These differences are sufficient to fix the structure parameters quite precisely.

these displacements with greater precision so as to test the proposal that the oxygen octahedron remains comparatively undistorted as in the cubic–tetragonal transition.

For this and the following experiment, the $KNbO_3$ powder was sealed in a vanadium can of approximately the same dimensions as the silica tube, and fixed in a cryostat having aluminium windows. The background scatter from this arrangement does not contain any peaks because of the small scattering length of vanadium and the large diameter of the aluminium window. The profile for the orthorhombic phase (figure 2) was collected in 22 hours at room temperature. At low scattering angles the profiles for the different phases are rather similar, but at high angles there are marked differences as the splitting of the aristotype peaks becomes more pronounced. On closer examination of larger scale drawings, the differences became apparent even at low angles. For example some peaks are broadened because two or more closely spaced reflexions contribute, and the intensity on one side of these peaks may fall more rapidly than on the other because of differences in the strength of these reflexions. The profile refinement procedure makes use of these systematic differences, so that even when the splitting is not resolved at all, information is extracted from the detailed shape of the peaks. At high angles the number of reflexions becomes so great that the observed peaks cannot be identified with specific reflexions at all, but the complex pattern is easily explained when the contributions of all reflexions are added up. More than twenty reflexions contribute to the intensity observed at some points, and more than 200 reflexions contribute to the complete profile for the orthorhombic phase.

The orthorhombic *Amm*2 cell contains two $KNbO_3$ units; in terms of the lattice dimensions a_0 and directions $[hkl]$ of the cubic aristotype, it has the dimensions $a = 3{\cdot}973$ Å $\simeq a_0$ along $\boldsymbol{x} = [100]$, $b = 5{\cdot}695$ Å $\simeq \sqrt{2}a_0$ along $\boldsymbol{y} = [0\bar{1}1]$ and $c = 5{\cdot}721$ Å $\simeq \sqrt{2}a_0$ along $\boldsymbol{z} = [011]$. The atomic coordinates for this cell are then

K at $0, 0, \Delta_z(\mathrm{K})$	$0, \frac{1}{2}, \frac{1}{2} + \Delta_z(\mathrm{K})$
Nb at $\frac{1}{2}, 0, \frac{1}{2} + \Delta_z(\mathrm{Nb})$	$\frac{1}{2}, \frac{1}{2}, \Delta_z(\mathrm{Nb})$
O_I at $0, 0, \frac{1}{2} + \Delta_z(O_I)$	$0, \frac{1}{2}, \Delta_z(O_I)$
O_{II} at $\frac{1}{2}, \frac{1}{4} + \Delta_y(O_{II}), \frac{1}{4} + \Delta_z(O_{II})$	$\frac{1}{2}, \frac{3}{4} + \Delta_y(O_{II}), \frac{3}{4} + \Delta_z(O_{II})$
O_{III} at $\frac{1}{2}, \frac{3}{4} - \Delta_y(O_{II}), \frac{1}{4} + \Delta_z(O_{II})$	$\frac{1}{2}, \frac{3}{4} - \Delta_y(O_{II}), \frac{3}{4} + \Delta_z(O_{II})$.

Again one of the parameters (we chose $\Delta_z(\mathrm{Nb})$) is determined by the requirement that the centre of mass is unmoved by these displacements $\Delta(\kappa)$.

The refinement proceeded as for the tetragonal phase, starting with various combinations of signs for the $\Delta(\kappa)$. With isotropic B-factors, a minimum R-factor of 2·35 was achieved, and this reduced to $R = 2{\cdot}11$ when anisotropic B-factors were introduced. These low R-factors represent exceptionally good fits to the data; in fact the difference between the observed and calculated points over the entire pattern closely approaches that expected for purely statistical fluctuations in the counts recorded. As for the tetragonal structure, the uncertainty in the value for the displacement $\Delta(\mathrm{K})$ of the potassium atom is increased if anisotropic B-factors are permitted, because of the high correlation (0·91) between $\Delta(\mathrm{K})$ and $B_{33}(\mathrm{Nb})$. However, the precision with which the displacement parameters have been obtained is most gratifying. The agreement with the x-ray work, where the standard deviations for the parameters appear to have been underestimated, is satisfactory considering the difficulties involved in single-crystal measurements. The present work does show, though, that the oxygen octahedra are less distorted than was indicated by the x-ray results. This is an important guide to the relative strengths

of the interatomic bonds, and brings the orthorhombic results into line with those obtained for the tetragonal phase. Again, the mean-square displacements of the oxygen atoms appear to be strongly anisotropic, but the estimated errors are relatively large for these parameters.

5. Orthorhombic–rhombohedral transition

The temperature of the cryostat was lowered to that of liquid nitrogen and then raised to 230 K for measurements on the rhombohedral phase: this is well below the transition temperature of 263 K, and the changes to the diffraction pattern (figure 3) are quite marked. The profile is less complex because now only about 110 separate reflexions

Table 3. Powder results for the rhombohedral $R3m$ phase at 230 K. $\Delta_x(K, Nb) = \Delta_y(K, Nb) = \Delta_z(K, Nb)$ while $\Delta_x(O_I) = \Delta_y(O_I) \simeq \Delta_z(O_I)$ with cyclic permutations for the equivalent O_{II} and O_{III}; the displacements are therefore almost purely along the [111] direction of the aristotype, with very little distortion of the oxygen octahedron.

		Powder, neutron $\lambda = 1{\cdot}0375$ Å				
	Isotropic $B(\kappa)$	Anisotropic $B_{ij}(\kappa)$				
$R_I \simeq 2R_F$	2·74	2·58				
$\Delta_z(K)$	0·0112 ± 25	0·0130 ± 81				*a*Å
$\Delta_z(Nb)$	0	0				*a*Å
$\Delta_x(O_I)$	0·0295 ± 5	0·0301 ± 9				*a*Å
$\Delta_z(O_I)$	0·0308 ± 7	0·0333 ± 15				*a*Å
	$B(\kappa)$	B_{ji}	B_{ji}	B_{ji}	$\bar{B}_{jj}(\kappa)$	
$B_{jj}(K)$	0·49 ± 5	0·51	0·51 ± 14	0·51	0·51	Å²
$B_{ji}(K)\ i \neq j$	0	0·16	0·16 ± 19	0·16		Å²
$B_{jj}(Nb)$	0·15 ± 5	0·15	0·15 ± 15	0·15	0·15	Å²
$B_{ji}(Nb)\ i \neq j$	0	0·10	0·10 ± 15	0·10		Å²
$B_{jj}(O_I)$	0·34 ± 3	0·46	0·46 ± 16	0·16 ± 11	0·37	Å²
$B_{ji}(O_I)\ i \neq j$	0	0·15 ± 19	0·10 ± 14	0·10		Å²
$a = b = c$	4·016	4·016				Å
$\alpha = \beta = \gamma$	89·818 ± 8	89·817 ± 9				
b_K	0·37	0·37				
b_{Nb}	0·69	0·69				
b_O	0·577	0·577				
N_{param}	14	19				
Time	1 day	1 day				

contribute. The rhombohedral cell can be described as a slight stretching of the aristotype cubic cell along [111], giving lattice constants of $a = b = c = 4{\cdot}016$ Å and $\alpha = \beta = \gamma = 89{\cdot}83°$ (Shirane *et al* 1954). The space group is $R3m$ (No 160), with atoms

K at $\Delta_z(K)$, $\Delta_z(K)$, $\Delta_z(K)$

Nb at $\frac{1}{2} + \Delta_z(Nb)$, $\frac{1}{2} + \Delta_z(Nb)$, $\frac{1}{2} + \Delta_z(Nb)$

O_I at $\frac{1}{2} + \Delta_x(O_I)$, $\frac{1}{2} + \Delta_x(O_I)$, $\Delta_z(O_I)$

O_{II} at $\frac{1}{2} + \Delta_x(O_I)$, $\Delta_z(O_I)$, $\frac{1}{2} + \Delta_x(O_I)$

O_{III} at $\Delta_z(O_I)$, $\frac{1}{2} + \Delta_x(O_I)$, $\frac{1}{2} + \Delta_x(O_I)$.

$\Delta_x(O_I) = \Delta_z(O_I)$ if the oxygen octahedron is undistorted, and $\Delta_z(Nb)$ is fixed in terms of the other $\Delta(\kappa)$ by the requirement that the centre of mass is unmoved. No previous work has been done to determine these displacements.

Refinement with isotropic B-factors yielded a minimum R-factor of 2·74, which was reduced to $R = 2{\cdot}58$ on inclusion of anisotropic B-factors. In either case we find once more that the oxygen octahedron moves as an essentially rigid unit against the potassium and niobium atoms. The increase in the uncertainty of the value of $\Delta(\kappa)$ when anisotropic B-factors are permitted is again due to the very large correlation (0·98) between $\Delta(\kappa)$ and $B_{ii}(Nb)$, although correlation between $\Delta(K)$ and the temperature factors of the other atoms also becomes important. Even with isotropic B-factors, the correlation between $\Delta(K)$ and $B(Nb)$ is high (0·91). The mean-square displacement of the oxygen atoms is even more anisotropic since $B_{11}(O_I) \simeq 3B_{33}(O_I)$. We expect this anisotropy to increase as we lower the temperature if it is due, as we suppose, to soft oxygen octahedra rotation modes, since the frequencies of these modes will decrease with temperature.

The precision with which we have determined the cell angle $\alpha = \beta = \gamma = 89{\cdot}817 \pm 0{\cdot}009$ degrees lends additional support to our claim that the lattice constants can be measured very precisely using the neutron powder profile technique.

6. The atomic displacements and spontaneous polarization for the different phases

The $\Delta(K)$ are the displacement coordinates for axes defined by the unit cell edges: except for the rhombohedral phase these axes are orthogonal, so that the actual displacements $\delta(\kappa)$ parallel to and perpendicular to the various ferroelectric axes are simply obtained by multiplying the $\Delta(K)$ by the appropriate lattice dimensions. These displacements, in Å, are given in table 4, with the origin chosen so that the centre of mass is unmoved. (The values of $\Delta(\kappa)$ obtained for the refinement with anisotropic B-factors have been used.) Table 4 also gives the values calculated for the spontaneous polarization $P_s = (e/v_c)\,\Sigma\, Z''_\kappa \delta_{\|}(\kappa)$ using these displacements (Cochran 1960). The apparent ionic charges Z''_κ, which allow for the contribution from the ionic polarizability, have been estimated (Hewat 1973a) from calculations of the lattice dynamics and infrared dipole

Table 4. Atomic displacements parallel ($\delta_{\|}(\kappa)$) and perpendicular ($\delta_{\perp}(\kappa)$) to the ferroelectric axis [ ] for the distorted phases of $KNbO_3$. These displacements are used, with the apparent ionic changes Z''_κ, to calculate the spontaneous polarization

$$P_s(\text{calc}) = \frac{e}{v_c} \sum_{\kappa} Z''_\kappa \delta_{\|}(\kappa)$$

for comparison with the measurements P_s(obs) of Triebwasser (1956).

	Tetragonal [001]	Orthogonal [011]	Rhombohedral [111]	
$\delta_{\|}(K)$	−0·014 ± 26	−0·009 ± 40	−0·013 ± 32	Å
$\delta_{\|}(Nb)$	0·063	0·070	0·078	Å
$\delta_{\|}(O_I)$	−0·117 ± 4	−0·138 ± 6	−0·140 ± 4	Å
$\delta_{\|}(O_{II}) \equiv$	−0·099 ± 3	−0·125 ± 4	−0·140	Å
$\delta_{\|}(O_{III})$	−0·099	−0·125	−0·140	Å
$\delta_{\perp}(O_I)$	0	0·014 ± 5	0·010 ± 8	Å
P_s(calc)	32 ± 4	38 ± 4	42 ± 4	$\mu C\,cm^{-1}$
P_s(obs)	30 ± 2	32 ± 3	NA	$\mu C\,cm^{-1}$

strengths of perovskites as $Z''_K = 1{\cdot}8 \pm 0{\cdot}3$, $Z''_{Nb} = 7{\cdot}5 \pm 1{\cdot}2$ and $Z''_O = -3{\cdot}1 \pm 0{\cdot}3$ electrons. Quite good agreement with Triebwasser's (1956) measurements of P_s(obs) is then obtained.

Figure 4 illustrates the different phase transitions of $KNbO_3$. The rigid oxygen octahedron is displaced first along [001] in the tetragonal phase (*a*), then along [011] in the orthorhombic phase (*b*), and finally along [111] in the rhombohedral phase (*c*).

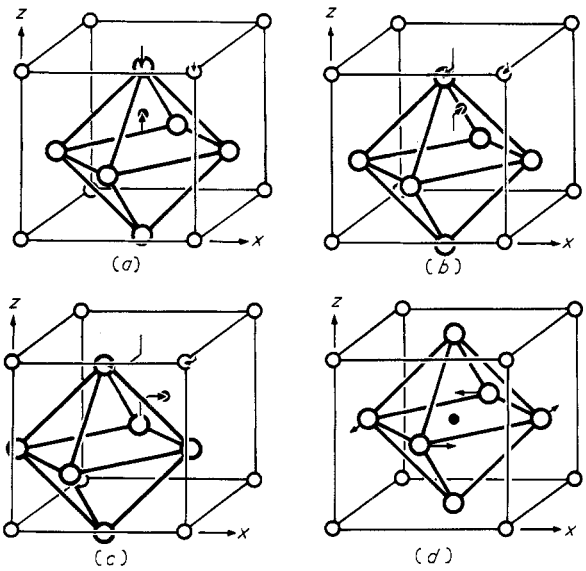

Figure 4. Atomic displacements from the cubic perovskite aristotype positions for the various phases of potassium niobate (centre of mass undisplaced). (*a*) tetragonal phase, (*b*) orthorhombic phase, and (*c*) rhombohedral phase. In these phase transitions, the oxygen octahedron is displaced as a rigid unit along (*a*) [001], (*b*) [011] and finally (*c*) [111]. These displacements have been greatly exaggerated in the drawings: for example the niobium atom does not actually move outside the oxygen octahedron as it appears to in figure (*c*). Drawing (*d*) shows how this rigid oxygen octahedron 'librates' in one of the unstable zone-boundary modes. These low-frequency librations mean that the oxygen atoms have relatively large mean-square displacements on the faces of the distorted cube. (○ potassium, ● niobium, ○ oxygen).

The last drawing (*d*) shows the oxygen octahedron librating in one of the low-frequency zone-boundary modes responsible for the observed anisotropy in the mean-square displacement of the oxygen atoms.

7. Conclusion

The profile refinement technique, when applied to neutron powder diffraction patterns, proves to be a powerful method for the precise measurement of the changes that occur when a crystal undergoes a structural transition. The results of this technique rival in precision those of the most careful single crystal experiments with either neutrons or x-rays, and yet can be obtained for a fraction of the time and effort required for single-crystal work. Because of this saving in time and effort, and because powdered samples

are much more readily available than are single crystals, the profile refinement of neutron powder patterns can compete strongly with other techniques for the structure refinement of moderately complex crystals for which approximate structures are already available. Indeed new possibilities are created for the comparative study of groups of materials under controlled conditions of temperature and pressure.

The results presented in this paper for the cubic–tetragonal–orthorhombic–rhombohedral transitions in potassium niobate illustrate the power of the technique. The results are, though, of interest in themselves, since this is the first time that such a long series of ferroelectric transitions in the one material has been studied systematically. They show that the oxygen octahedron in $KNbO_3$ can be regarded as an essentially rigid unit, having low-frequency vibrational and librational modes, the former condensing to produce the ferroelectric distortions observed in the low-temperature phases, the latter being revealed in the large anisotropy of the mean-square displacements of the oxygen atoms.

Acknowledgments

Dr H M Rietveld of the Reactor Centrum Nederland provided a copy of his original profile refinement computer program, and Dr J B Forsyth of the Rutherford Laboratory helped to compile the program on the IBM 370 system. Dr B T M Willis of Harwell gave continued encouragement and advice, and offered constructive criticism of this paper.

References

Cochran W 1960 *Adv. Phys.* **9** 387–423
Cowley R A *Phys. Rev.* **134** A981–97
Glazer A and Megaw H D 1972 *Phil. Mag.* **25** 1119–35
Hewat A W 1972 *Phys. Stat. Solidi* (b) **53** K33–5
—— 1973a *J. Phys.* C: *Solid St. Phys.* **6** 1074–84
—— 1973b *UKAEA Research Group Report* (unpublished)
Katz L and Megaw H D 1967 *Acta Crystallogr.* **22** 639–48
Rietveld H M 1969 *J. appl. Crystallogr.* **2** 65–71
Shirane G, Danner H, Pavlovic A and Pepinsky R 1954 *Phys. Rev.* **93** 672–3
Triebwasser S 1956 *Phys. Rev.* **101** 993–7
Wilson A J C 1963 *Mathematical Theory of X-ray powder Diffractometry* (Amsterdam: Philips Techn. Library)